

EXCITATION OF A PULSE ELECTROMECHANICAL CONVERTER OF ELECTRODYNAMIC TYPE FROM A TWO-SECTION CAPACITOR ENERGY STORAGE

V.F. Bolyukh*

National Technical University "Kharkiv Polytechnic Institute",
st. Kirpicheva, 2, Kharkov, 61002, Ukraine, e-mail: vfolyukh@gmail.com

A mathematical model of a pulsed electromechanical converter (PEC) of electrodynamic type has been developed, in which the solutions of the equations are presented in a recurrent form, which, when numerically implemented, allows taking into account the interrelated electrical, magnetic, mechanical and thermal processes and their nonlinear parameters. While maintaining the total energy of the pulsed source, the influence of the distribution of energy between the two sections of the capacitive energy storage (CES) and the voltage at which the additional section of the CES is connected was established. When operating in an accelerating mode, the largest amplitude of electrodynamic forces (EDF) and maximum speed occur in the basic version of the PEC, which is excited only from the main section of the CES, and the most effective is the PEC with the smallest capacity of the main section of the CES, and its maximum value is 2.61 higher than for the basic version of the PEC. When operating in the shock-power mode, compared with the basic version of the PEC, the amplitude of the EDF decreases. The most effective is the PEC with the smallest capacity of the main section of the CES, and its maximum value is 5.17 higher than that of the basic version of the PEC. Experimental studies of the PEC in the shock-power mode established that the oscillograms of the voltage of the CES and the current of the PEC correspond to the calculated characteristics, and their main indicators are consistent with each other with an accuracy of 5-7%. References 16, figures 6.

Key words: pulse electromechanical converter of electrodynamic type, mathematical model, two sections of capacitive energy storage, efficiency criterion, experimental research.

Introduction. Pulse electromechanical converters (PEC) with a linear movement of the armature are used to create powerful power pulses and ensure high speeds [1, 2]. One of the most effective is an electrodynamic type PEC with two coaxially mounted disc windings [3]. The stationary winding, which performs the function of an inductor, is electrically connected in series and opposite to the magnetic field with a movable winding, which serves as an armature and acts on the actuator. The armature is connected to the inductor and to the switching power supply with the help of flexible current leads, which contains a capacitive energy storage (CES). PEC, when operating in accelerating mode, provides a high speed of the actuator in a short active section, and when operating in shock-power mode, it provides significant force impulses to the object of influence with a slight displacement of the actuator.

PEC are used in various technical, scientific and test systems. PEC are used in electromagnetic hammers and rock drills, in devices for driving piles, in rock separators and vibrators, in seismic sources for exploration, in presses with a wide range of impact energies, in vibrating mixers and dispensers for the chemical and biomedical industries, in magnetic pulse devices for shock pressing of ceramics powders, in shock-mechanical devices for cleaning containers from adhesion of bulk materials, in devices for destroying information on digital media, in high-speed electrical devices and valve-switching equipment, in devices for smooth damping and stopping of movable actuators, in test complexes for testing products for shock loads, in catapults of unmanned aerial vehicles, in throwing devices for extinguishing fires, in aerospace and defense systems, etc. [4-9].

Compared to PEC of induction and electromagnetic types, electrodynamic type converters, despite their more complex design due to flexible current leads and an armature made in the form of a multi-turn disk winding, have higher electromechanical performance [10, 11]. However, for more efficient operation, it is necessary to provide increased indicators of the PEC of the electrodynamic type. So, when using a low-voltage CES, charged at a voltage of 300 V, when operating in an accelerating mode, it is necessary to develop a speed of 10-13 m/s in 1 ms, and when operating in a shock-power mode, the magnitude of the EDF impulse is 10-13 N·s. The indicated indicators must be ensured at relatively low values of the amplitudes of the excitation current (up to 1.5 kA) and electrodynamic forces (up to 15 kN). This is due to the fact that a significant amplitude of the excitation current determines the use of electronic devices with increased operating parameters in a pulsed power supply. And a significant amplitude of electrodynamic forces (EDF) acting on the inductor causes an increased return of the converter. Recoil reduces the speed of the actuator when

operating in accelerating mode and the force impact on the object when operating in shock-power mode. This limits the scope of the considered converter. So, in a ballistic laser gravimeter, an induction-dynamic catapult should provide the maximum height of the actuator toss with a minimum recoil of the stationary inductor [12].

For PEC, the most expedient is the excitation scheme with a polar aperiodic pulse, in which electrolytic capacitors with increased energy performance can be used. Of particular interest is a circuit with sequential excitation of the PEC from two sections of the CES, in which the additional section is charged at a reduced voltage in relation to the main section [13]. Note that if the inductor in a PEC of induction type is made in the form of axially located sections of a solenoidal configuration, inside which an armature of a similar configuration moves, then with sequential excitation from a multisection CES the efficiency of the electromechanical accelerator increases [14]. However, if in such a converter the inductor and the armature have a disk configuration, then such excitation is not possible.

In works [15, 16] it is shown that the additional section of the CES increases the performance of the PEC, in which the inductor and the armature have a disk configuration, but this is due to the increased energy of the pulsed source. Of interest is the option of two-section excitation of the PEC while maintaining the total energy of the pulsed source $W_{\Sigma} = W_0 + W_1$, where $W_0 = 0.5C_0U_0^2$ is the energy of the main section of the CES, $W_1 = 0.5C_1U_1^2$ is the energy of the additional section of the CES. This raises the question of the influence of the parameters of the CES sections of the pulsed source on the efficiency indicators of the PEC of the electrodynamic type.

The purpose of the article is to determine the influence of the distribution of energy between two sections of the CES and the voltage at which an additional section of the CES is connected, while maintaining the total energy of the pulsed source, on the efficiency indicators of the PEC of the electrodynamic type when operating in accelerating and shock-force modes of operation.

Let us consider a converter in which a fixed inductor 1 and a movable armature 2 are made in the form of coaxially installed disc windings (Fig. 1). The inductor is connected to a fixed stop 3, and the armature interacts with the actuator 4. The inductor and the armature are tightly wound in two rows with a copper bus, which has an internal bend from one row to another, and impregnated with epoxy resin. Due to this design, the leads of the inductor and the armature are located in the outer layers, which makes it easy to connect them both to a switching power supply and to each other. The armature is connected to the inductor and to the power supply using flexible current leads q_1, q_2 .

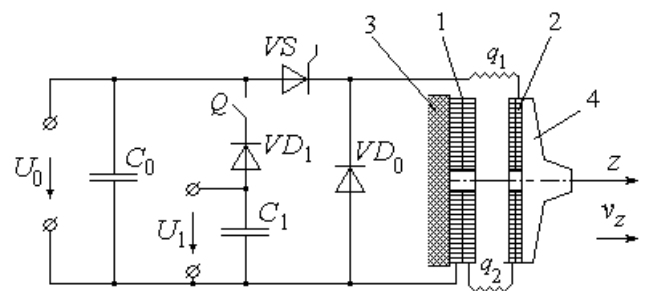


Fig. 1

The constant polarity of the excitation current pulse is provided by the reverse diode VD_0 , and the thyristor VS starts the PEC into operation. When the Q key is open, the PEC is excited only from the main section of the CES with a capacitance C_0 , which is charged to a voltage U_0 . With the closed key Q , when the voltage of the main section of the CES becomes $u_c = U_1$, an additional section of the CES with a capacitance C_1 is connected to it with the help of the VD_1 diode, and the capacitance of the pulse source becomes equal $C_{\Sigma} = C_0 + C_1$.

The constant polarity of the excitation current pulse is provided by the reverse diode VD_0 , and the thyristor VS starts the PEC into operation. When the Q key is open, the PEC is excited only from the main section of the CES with a capacitance C_0 , which is charged to a voltage U_0 . With the closed key Q , when the voltage of the main section of the CES becomes $u_c = U_1$, an additional section of the CES with a capacitance C_1 is connected to it with the help of the VD_1 diode, and the capacitance of the pulse source becomes equal $C_{\Sigma} = C_0 + C_1$.

We will assume that when operating in the accelerating mode, the armature moves strictly axially together with the actuator, and when operating in the shock-force mode, the armature does not move. We assume that all semiconductor devices have zero resistance in the forward direction and zero conductance in the opposite direction. We neglect the resistance of the connecting wires.

Mathematical model of PEC. Let us consider a mathematical model of an PEC of an electrodynamic type in an accelerating mode of operation, since there is a change in the magnetic connection between the active elements - an inductor and an armature, while in the shock-force mode this connection is unchanged. We will consider the interrelated electromagnetic, mechanical and thermal processes using a model that uses the lumped parameters of active elements. Let us represent the solutions of the equations in a recurrent form, which, when numerically implemented, makes it possible to take into account interrelated processes of various nature and nonlinear parameters.

Electromagnetic processes in the PEC during a discharge from the main section of the CES with parameters C_0, U_0 on the interval $\{0, t_1\}$, where t_1 is the time at which the voltage of the CES $u_C=0$, can be described by the equation [11]:

$$[R_1(T_1) + R_2(T_2)] \cdot i + \frac{d\psi}{dt} + \frac{1}{C_0} \int_0^t idt = 0, \quad u_C = \frac{1}{C_0} \int_0^t idt = U_0, \quad (1)$$

where $n=1, 2$ are the indices of the inductor and the armature, respectively; R_n, T_n are the active resistance and temperature of the n -th active elements; i is the excitation current; u_C is the voltage of the CES;

$$\frac{d\psi}{dt} = [L_1 - 2M_{12}(z) + L_2] \frac{di}{dt} - 2iv_z(t) \frac{dM_{12}}{dz}, \quad (2)$$

L_n is the inductance of the n -th active element; M_{12} is the mutual inductance between the inductor and the armature, which moves along the z -axis at a speed v_z .

Substituting equation (2) into (1) we obtain:

$$(R^* - \Xi) \cdot i + [L^* - 2M_{12}(z)] \frac{di}{dt} + \frac{1}{C_0} \int_0^t idt = 0, \quad (3)$$

where $R^* = R_1(T_1) + R_2(T_2)$; $L^* = L_1 + L_2$; $\Xi = 2v_z(t) \frac{dM_{12}}{dz}$.

The solution to equation (3) is presented in the form:

$$i = A_1 \exp(\alpha_1 t) + A_2 \exp(\alpha_2 t), \quad (4)$$

where A_1, A_2 are the arbitrary constants;

$\alpha_{1,2} = \left\langle \pm \left\{ 0.25[R^* - \Xi]^2 - [L^* - 2M_{12}(z)]C_0^{-1} \right\}^{0.5} + 0.5(R^* - \Xi) \right\rangle (2M_{12}(z) - L^*)^{-1}$ are the roots of the characteristic equation.

To represent the solution in a recurrent form, we define the values of arbitrary constants A_1 and A_2 at the time t_k .

If $(R^* - \Xi) > 2\sqrt{[L^* - 2M_{12}(z)]C_0^{-1}}$, then after a series of transformations we get:

$$A_{1,2} = \frac{u_C(t_k) + (R^* - \Xi)i(t_k) + \alpha_{2,1} \cdot i(t_k)[L^* - 2M_{12}(z)]}{[L^* - 2M_{12}(z)] \exp(\alpha_{1,2} t_k) (\alpha_{2,1} - \alpha_{1,2})}. \quad (5)$$

Substituting expressions (5) into equation (4), we obtain the expression for the current:

$$i(t_{k+1}) = \frac{u_C(t_k) + (R^* - \Xi)i(t_k)}{[L^* - 2M_{12}(z)](\alpha_2 - \alpha_1)} [\exp(\alpha_1 \Delta t) - \exp(\alpha_2 \Delta t)] + \frac{i(t_k)}{\alpha_2 - \alpha_1} [\alpha_2 \exp(\alpha_1 \Delta t) - \alpha_1 \exp(\alpha_2 \Delta t)], \quad (6)$$

where $\Delta t = t_{k+1} - t_k$.

The voltage on the CES is described by the equation:

$$u_C(t_{k+1}) = \frac{u_C(t_k) + (R^* - \Xi)i(t_k)}{\alpha_2 - \alpha_1} [\alpha_2 \exp(\alpha_1 \Delta t) - \alpha_1 \exp(\alpha_2 \Delta t)] + \frac{[L^* - 2M_{12}(z)]i(t_k)}{\alpha_2 - \alpha_1} [\alpha_2^2 \exp(\alpha_1 \Delta t) - \alpha_1^2 \exp(\alpha_2 \Delta t)]. \quad (7)$$

If $(R^* - \Xi) < 2\sqrt{[L^* - 2M_{12}(z)]C_0^{-1}}$, then the roots of the characteristic equation can be represented in complex form:

$$\alpha_{1,2} = -\delta \pm j\omega_1 = \omega_0 \exp(j(\pi \pm \theta)), \quad (8)$$

where $\delta = 0.5 \frac{R^* - \Xi}{L^* - 2M_{12}(z)}$; $\omega_0 = [C_0(L^* - 2M_{12}(z))]^{0.5}$; $\theta = \arctg \left(4 \frac{L^* - 2M_{12}(z)}{C_0(R^* - \Xi)^2} - 1 \right)^{0.5}$;

$$\omega_1 = \left(\frac{1}{C_0(L^* - 2M_{12}(z))} - \left(\frac{R^* - \Xi}{2[L^* - 2M_{12}(z)]} \right)^2 \right)^{0.5}.$$

Substituting the values of the roots (8) into equations (6) and (7) and taking into account that $2j \sin(\omega_1 \Delta t) = \exp(j\omega_1 \Delta t) - \exp(-j\omega_1 \Delta t)$, we obtain:

$$i(t_{k+1}) = -\omega_1^{-1} \exp(-\delta\Delta t) \left\{ \frac{u_C(t_k) + (R^* - \Xi) \cdot i(t_k)}{L^* - 2M_{12}(z)} \sin(\omega_1\Delta t) + \omega_0 i(t_k) \sin(\omega_1\Delta t - \theta) \right\}. \quad (9)$$

$$u_C(t_{k+1}) = -\omega_0 \omega_1^{-1} \exp(-\delta\Delta t) \left\{ [u_C(t_k) + (R^* - \Xi) \cdot i(t_k)] \sin(\omega_1\Delta t - \theta) + i(t_k) \omega_0 (L^* - 2M_{12}(z)) \sin(\omega_1\Delta t - 2\theta) \right\}. \quad (10)$$

If $(R^* - \Xi) = 2\sqrt{(L^* - 2M_{12}(z))C_0^{-1}}$, then $\delta = \omega_0$. In this case, the current is described by the expression:

$$i(t_{k+1}) = \left\{ i(t_k) \delta - (L^* - 2M_{12}(z))^{-1} [u_C(t_k) + (R^* - \Xi) \cdot i(t_k)] \right\} \exp(-\delta\Delta t) \Delta t, \quad (11)$$

and the voltage on the CES is described by the expression:

$$u_C(t_{k+1}) = [u_C(t_k) - i(t_k)(L^* - 2M_{12}(z))\delta + (R^* - \Xi) \cdot i(t_k)] \left\{ \delta\Delta t + 1 \right\} \exp(-\delta\Delta t) + i(t_k) \left\{ (L^* - 2M_{12}(z))\delta - R^* + \Xi \right\}. \quad (12)$$

The current in the PEC on the time interval $\{t_1, \infty\}$, flowing through the diode VD_0 , is described by the equation:

$$i(t_{k+1}) = i(t_k) \exp\left(\frac{(\Xi - R^*)\Delta t}{L^* - 2M_{12}(z)}\right). \quad (13)$$

The mechanical processes of a PEC of electrodynamic type when operating in an accelerating mode can be described by the equation:

$$f_z(t, z) = (m_a + m_2) \frac{dv_z}{dt} + K_p h_z(t) + K_T v_z(t) + 0,125\pi\gamma_a \beta_a D_{2m}^2 v_z^2(t), \quad (14)$$

where $f_z(t, z) = i^2(t) \frac{dM_{12}}{dz}(z)$ is the instantaneous value of axial EDF acting between active elements; m_2 , m_a is the mass of the armature and actuator, respectively; K_p is the coefficient of elasticity of the buffer element (return spring); $h_z(t)$ is the amount of movement of the armature with the actuator; K_T is the coefficient of dynamic friction; γ_a is the density of the moving medium; β_a is the coefficient of aerodynamic resistance; D_{2m} is the outer diameter of the actuator.

Based on equation (14), the amount of movement of the armature with the actuator can be represented in the form of a recurrent relation:

$$h_z(t_{k+1}) = h_z(t_k) + v_z(t_k)\Delta t + g\Delta t^2 / (m_a + m_2), \quad (15)$$

where $v_z(t_{k+1}) = v_z(t_k) + g\Delta t / (m_a + m_2)$ is the speed of the armature with the actuator along the z -axis;

$$g = i^2(t_k) \frac{dM}{dz}(z) - K_p \Delta z(t_k) - K_T v_z(t_k) - 0,125\pi\gamma_a \beta_a D_{2m}^2 v_z^2(t_k)$$

When the PEC is operating in the shock-power mode, there is no armature movement and the EDF $f_z(t) = i^2(t) \frac{dM_{12}}{dz}$ acts on it.

Thermal processes. When the PEC is operating in the shock-power mode, thermal interaction occurs between its active elements through an insulating gasket. Their temperatures can be described by the recurrence relation:

$$T_n(t_{k+1}) = T_n(t_k) \zeta + (1 - \zeta) \left[\pi^{-1} i_n(t_k) R_n(T_n) (D_{en}^2 - D_{in}^2)^{-1} + 0,25\pi T_0 D_{en} H_n \alpha_{Tn} + T_m(t_k) \lambda_a(T) d_a^{-1} \right] \left\{ 0,25\pi \alpha_{Tn} D_{en} H_n + \lambda_a(T) d_a^{-1} \right\}^{-1}, \quad (16)$$

where $\zeta = \exp\left\{ -\frac{\Delta t}{C_n(T_n) \gamma_n} \left(0,25 D_{en} \alpha_{Tn} + \frac{\lambda_a(T)}{d_a H_n} \right) \right\}$; $\lambda_a(T)$ is the thermal conductivity coefficient of the insulation pad; d_a is the thickness of the gasket; D_{en} , D_{in} is the external and internal diameters of active elements, respectively; α_{Tn} is the heat transfer coefficient of the n -th active element; C_n is the heat capacity of the n -th active element.

When the PEC is operating in an accelerating mode and the armature moves, the temperatures of the active elements, neglecting the heat transfer through the connecting flexible current lead, can be described by the recurrence relation:

$$T_n(t_{k+1}) = T_n(t_k) \chi + (1 - \chi) \left[T_0 + 4\pi^{-2} i_n(t_k) R_n(T_n) \alpha_{Tn}^{-1} D_{en}^{-1} H_n^{-1} (D_{en}^2 - D_{in}^2)^{-1} \right], \quad (17)$$

where $\chi = \exp\left\{ -0,25\Delta t D_{en} \alpha_{Tn} C_n^{-1}(T_n) \gamma_n^{-1} \right\}$.

The initial conditions for the mathematical model of the PEC are as follows: $u_c(0)=U_0$ is the voltage of the main section of the CES; $i(0)=0$ is the excitation current; $h_z(0)=h_{z0}$ is the axial distance between active elements; $v_z(0)=0$ is the armature speed along the axis z ; $T_n(0)=T_0$ is the temperature of the n -th active element.

In order to take into account the complex of interrelated electrical, magnetic, thermal and mechanical processes, which are described by nonlinear equations, and various nonlinear dependences, we use a computational iterative algorithm. The entire workflow is divided into a large number of small calculated time intervals $\Delta t = t_{k+1} - t_k$, within which all values are considered unchanged. At each calculated interval Δt the parameters and indicators of the PEC at the moment of time t_k are the initial for the calculation. These values are the starting point for calculating all quantities at a point in time t_{k+1} . The current and voltage values of the CES, presented in the form of recurrent relationships, are organically built into the calculation algorithm. The temperatures of the active elements T_n are calculated from the current i values obtained at the time instant t_{k+1} . After that, the parameters caused by temperature changes are determined, namely, active resistance $R_n(T_n)$ and heat capacity $C_n(T_n)$ of active elements, thermal conductivity coefficient of the insulating pad $\lambda_a(T_n)$. At the same time t_{k+1} the EDF $f_z(t)$ value is calculated. After that, when the PEC is operating in the accelerating mode, the speed v_z and displacement h_z , the armature, the mutual inductance M_{12} between the active elements are sequentially calculated. When the PEC is operating in the shock-power mode, the magnitude of the EDF impulse P_z is calculated. Obtained values at a point in time t_{k+1} are used to calculate the current i in the next time interval t_{k+2} and the calculation process is cyclically repeated. The size of the skin layer in active elements is estimated according to the results of the calculation and, if necessary, an iterative process of adjusting the resistance is carried out. With this approach, linear equations and ratios can be used to determine the excitation current at a small calculated time interval Δt . The size of the calculated step Δt is chosen so that it does not have a significant effect on the calculation results.

We will assume that the energy of the pulsed source $W_\Sigma = W_0 + W_1$ is unchanged, where $W_0 = 0.5C_0U_0^2$ is the energy of the main section of the CES, $W_1 = 0.5C_1U_1^2$ is the energy of the additional section of the CES. When operating in a shock-force mode, the PEC efficiency will be estimated by the magnitude of the EDF impulse $P_z = \int f_z(t)dt$ and a dimensionless criterion $K_p^* = P_z^* (f_m^* \cdot i_m^*)^{-1}$, and when operating in an accelerating mode, the PEC efficiency will be estimated by the maximum speed V_m and a dimensionless criterion $K_v^* = V_m^* (f_m^* \cdot i_m^*)^{-1}$. Here are indicated $P_z^*, V_m^*, f_m^*, i_m^*$ - the relative values of the EDF impulse, the maximum speed of the armature, the amplitude of the EDF and the excitation current, respectively. The relative values of the indicators are normalized by the corresponding indicators of the basic PEC, in which the windings are excited only from the main section of the CES.

The main parameters of the PEC. The outer and inner diameters of the n -th active element are $D_{en}=100$ mm and $D_{in}=10$ mm, respectively. The inductor is tightly wound with a copper bus section $a_1 \times b_1 = 1.2 \times 4.8$ mm² and its axial height is $H_1=10$ mm. The armature is tightly wound with a copper bus section $a_2 \times b_2 = 1.2 \times 2.4$ mm² and its axial height is $H_2=5$ mm. The initial distance between the active elements is $h_{z0}=1$ mm. When operating in an accelerating mode, an actuator with a mass of $m_a=0.25$ kg and a return spring with a coefficient of elasticity $K_p=250$ N/m are used. The energy of the impulse source $W_\Sigma=270$ J. The voltage of the main section of the CES is $U_0=300$ V. When the Q key is open, the PEC is excited only from the main section of the CES with a capacity of $C_0=6$ mF.

Electromechanical characteristics of PEC. Let us consider the influence of the voltage U_1 of the additional section of the CES, which we will evaluate by the value of the relative voltage $u_1^* = (U_0 - U_1)U_0^{-1}$, on the performance of the PEC. Let us consider the characteristics of an PEC operating in an accelerating mode when an additional section of the CES is connected, the energy of which is $W_1=W_0$. Compared with the basic version of the PEC, the source voltage u_c decreases faster until the moment of connecting the additional section of the CES (Fig. 2, *a*). When this section is connected, a kink is observed in the u_c voltage curves, after which the voltage decreases more slowly. The greater the relative voltage $u_1^* = (U_0 - U_1)U_0^{-1}$ of the additional section of the CES, and therefore the greater its capacity C_1 , the more pronounced the indicated effect. Compared with the basic version of the PEC, the amplitude of the excitation current pulse i decreases, and the duration of the trailing edge increases. A similar character is manifested for the EDF f_z : with a de-

crease in the value of the relative voltage u_1^* , the amplitude decreases, and the duration of the trailing edge increases (Fig. 2, b). Since the armature under the action of the EDF moves a distance h_z , the attenuation of the EDF occurs more significantly than the attenuation of the excitation current. The higher the relative voltage u_1^* , the lower the speed v_z developed by the PEC. The highest speed is developed in the basic PEC.

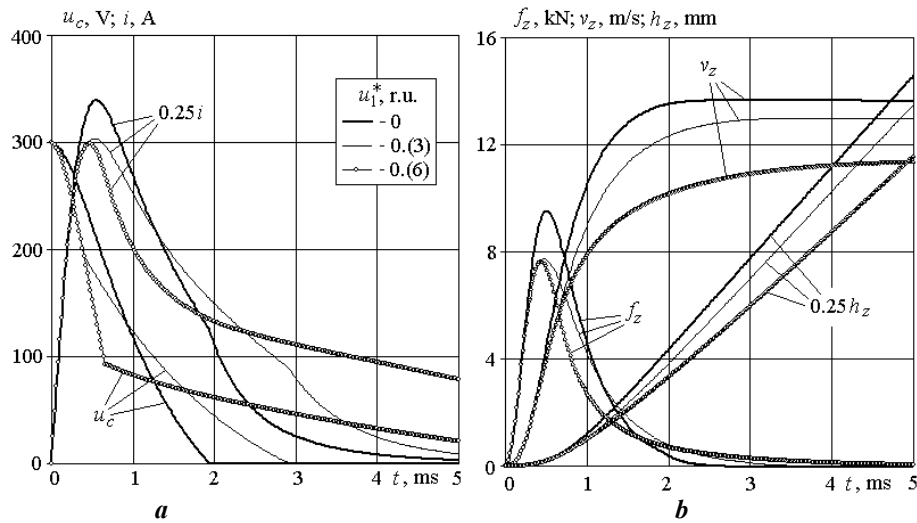


Fig. 2

Let us consider the effect of the relative voltage value u_1^* of the additional section of the CES on the PEC indicators for different capacities of the main section of the CES C_0 . The greatest amplitude of the EDF f_m and the maximum speed of the armature together with the actuating element V_m take place in the basic version of the PEC (Fig. 3, a, b). The larger the capacity of the main section of the CES, the higher the indicated indicators. With an increase in the relative voltage u_1^* , the maximum velocity V_m and the amplitude of the EDF f_m decrease. Moreover, the amplitude of the EDF f_m after a certain voltage value u_1^* remains unchanged. When operating in an accelerating mode, the connection of an additional section of the CES increases the efficiency criterion K_V^* in comparison with the basic version of the PEC (Fig. 3, c). The most effective is the PEC with the smallest capacity of the main section of the CES C_0 . Depending on the relative voltage u_1^* of the additional section of the CES, the efficiency criterion K_V^* has a pronounced maximum, which shifts to higher values u_1^* with a decrease in the capacitance C_0 . The highest value of the efficiency criterion $K_V^*=2.61$ occurs at $C_0=1$ mF and $u_1^*=0.6$.

Let us carry out similar studies of the PEC when operating in shock-power mode. In this mode of operation, the amplitude of the excitation currents is up to 20% higher, and the duration of the trailing edge is shorter than when the PEC is operating in the accelerating mode (Fig. 4, a). As a result, the amplitude of the EDF f_m increases to 50% (Fig. 4, b).

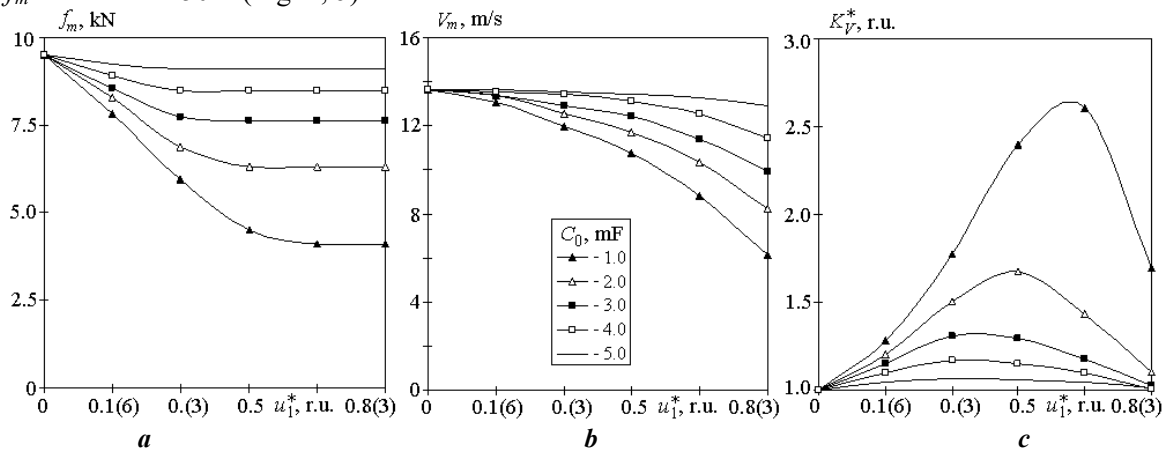


Fig. 3

Compared with the basic version of the PEC, the connection of an additional section of the CES with a relative voltage $u_1^*=0.(3)$ reduces the amplitude of the excitation current by 12%. So, at relative voltage $u_1^*=0.(6)$ the current amplitude decreases by 22.5%. Note that there is no such dependence when operating in the accelerating mode of PEC operation. At large values of the relative voltage u_1^* , the amplitude of the EDF decreases (Fig. 4, *b*). However, due to an increase in the duration of the trailing edge, the magnitude of the EDF impulse does not have an unambiguous relationship. So, the largest value of the EDF impulse $P_z=14.16$ N·s takes place in the PEC, in which the value of the relative voltage $u_1^*=0.(3)$, and the smallest value $P_z=13.63$ N·s occurs in the basic version of the PEC.

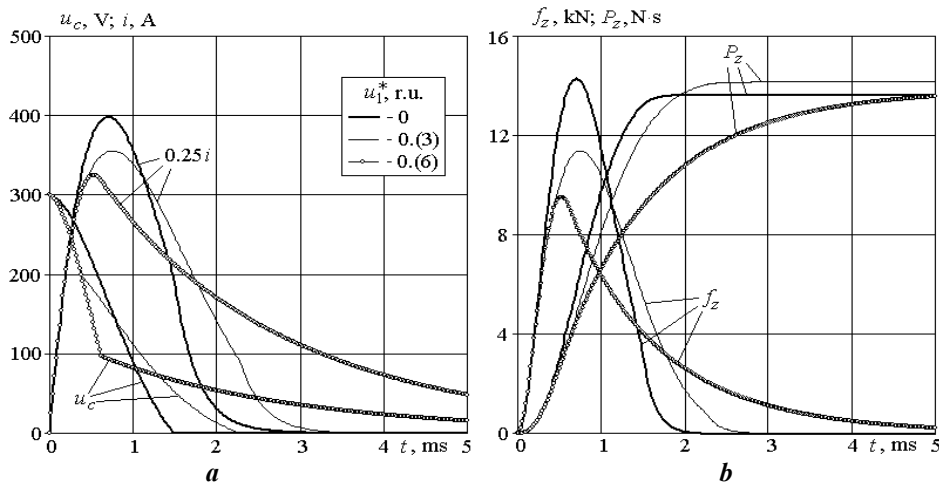


Fig. 4

Let us consider the influence of the relative voltage u_1^* of the additional section of the CES on the indicators of the PEC operating in the shock-power mode, with different capacities of the main section of the CES C_0 (Fig. 5). In comparison with the accelerating mode of operation of the PEC, in general, the nature of the change in the amplitude of the EDF f_m from the value of the relative voltage u_1^* remains, but with higher values (Fig. 5, *a*). In comparison with the basic version of the PEC, depending on the value of the relative voltage u_1^* , the magnitude of the EDF impulse P_z somewhat (up to 5%) increases at C_0 equal to 2 mF and 3 mF in the range of relative voltages $u_1^* \in (0, 0.5)$ (Fig. 5, *b*). And in the interval $u_1^* \geq 0.5$ at all values of C_0 , the magnitude of the EDF pulse P_z decreases.

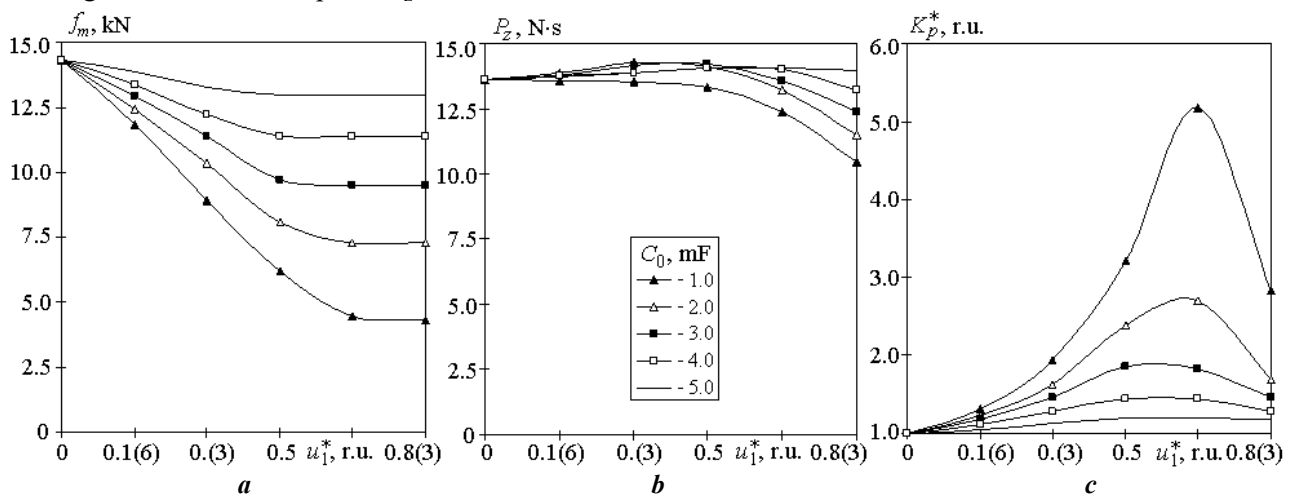


Fig. 5

Compared with the basic version of the PEC, operating in the shock-power mode, the connection of an additional section of the CES increases the efficiency criterion K_p^* (Fig. 5, *c*). The most effective is the PEC with the smallest capacity of the main section of the CES C_0 . Depending on the voltage of the additional section of the CES, the efficiency criterion K_p^* has a maximum, which shifts to higher values of the

relative voltage u_1^* as the capacitance C_0 decreases. The highest value of the efficiency criterion $K_p^* = 5.17$ occurs at $C_0 = 1$ mF and $u_1^* = 0$.(6).

To confirm the main calculated results, experimental studies of the PEC were carried out when operating in the shock-power mode. In the experiments, to the main section of the CES with parameters $C_0 = 2.2$ mF, $U_0 = 300$ V, an additional section of the CES was connected in two versions: 1) $C_1 = 2.2$ mF, $U_1 = 260$ V and 2) $C_1 = 6.6$ mF, $U_1 = 150$ V. In both versions, the total energy of the pulsed source is $W_\Sigma \approx 175$ J. Fig. 6 shows oscillograms of the voltage of the CES u_c and the current i of the PEC for version 1 (Fig. 6, a) and for version 2 (Fig. 6, b) of the additional section of the CES. From the presented oscillograms it can be seen that at a lower voltage U_1 the amplitude of the excitation current increases, and at a higher voltage U_1 the duration of the trailing edge of the excitation current increases. At the moment of connecting the additional section of the CES, a characteristic break is observed on the voltage curves of the CES u_c . At a lower voltage U_1 , the indicated kink is more pronounced, which corresponds to the calculated results. In general, the experimental oscillograms of the voltage of the CES u_c and the current i of the PEC when operating in the shock-power mode correspond to the calculated characteristics. The experimental and calculated indicators are consistent with each other with an accuracy of 5-7%, which indicates the reliability of the studies.

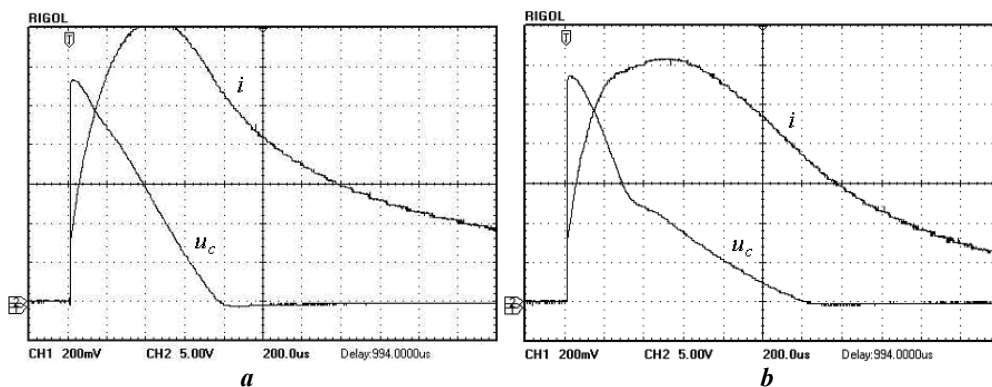


Fig. 6

Conclusions. 1. A mathematical model of an PEC of electrodynamic type has been developed, in which the solutions of the equations are presented in a recurrent form, which, when numerically implemented, allows taking into account the interrelated electrical, magnetic, mechanical and thermal processes and their nonlinear parameters.

2. While maintaining the total energy of the pulsed source, the influence of the distribution of energy between the two sections of the CES and the voltage at which an additional section of the CES is connected on the efficiency indicators of the PEC of the electrodynamic type with disk windings during operation in accelerating and shock-power modes of operation was established.

3. When operating in an accelerating mode, the greatest amplitude of the EDF and the maximum speed take place in the basic version of the PEC, which is excited only from the main section of the CES. Connecting an additional section of the CES increases the efficiency criterion of the PEC, which takes into account the relative values of the maximum armature speed, the amplitude of the EDF and the excitation current. The most efficient is the PEC with the smallest capacity of the main section of the CES, and its maximum value is 2.61 higher than that of the basic version of the PEC.

4. When operating in the shock-power mode, the amplitude of the EDF increases to 50% compared to the accelerating mode of operation. However, in comparison with the basic version of the PEC, the amplitude of the EDF decreases. Connecting an additional section of the CES increases the efficiency criterion, which takes into account the relative values of the EDF pulse, the EDF amplitude and the excitation current. The most effective is the PEC with the smallest capacity of the main section of the CES, and its maximum value is 5.17 higher than that of the basic version of the PEC.

5. Experimental studies of the PEC in the shock-power mode established that the oscillograms of the voltage of the CES and the current of the PEC correspond to the calculated characteristics, and their main indicators are consistent with each other with an accuracy of 5-7%.

The work was done on the state budget theme "Improvement of technical systems and devices due to impulse electromechanical converters and electrophysical technologies". State Registration Number: 0117U004881. (01/01/2017 - 31/12/2018).

1. McNab I.R. A research program to study airborne launch to space. *IEEE Transactions on Magnetics*. 2007. Vol. 43. No 1. Pp. 486-490. DOI: <https://doi.org/10.1109/TMAG.2006.887447>.
2. Kondratenko I.P., Zhiltsov A.V., Paschin M.O., Vasyuk V.V. Choice of parameters of induction electromechanical converter for electrodynamic processing of welded joints. *Tekhnichna Elektrodynamika*. 2017. No 5. Pp. 83-88. DOI: <https://doi.org/10.15407/techned2017.05.083>. (Ukr).
3. Bissal A., Magnusson J., Engdahl G. Comparison of two ultra-fast actuator concept. *IEEE Transactions on Magnetics*. 2012. Vol. 48. No 11. Pp. 3315-3318. DOI: <https://doi.org/10.1109/tmag.2012.2198447>.
4. Kondratiuk M., Ambroziak L. Concept of the magnetic launcher for medium class unmanned aerial vehicles designed on the basis of numerical calculations. *Journal of Theoretical and Applied Mechanics*. 2016. Vol. 54. Issue 1. Pp. 163-177. DOI: <https://doi.org/10.15632/jtam-pl.54.1.163>.
5. Angquist L., Baudoin A., Norrga S., Nee S., Modeer T. Low-cost ultra-fast DC circuit-breaker: Power electronics integrated with mechanical switchgear. *IEEE International Conference on Industrial Technology (ICIT)*. Lyon. 2018. Pp. 1708-1713. DOI: <https://doi.org/10.1109/ICIT.2018.8352439>.
6. Puumala V., Kettunen L. Electromagnetic design of ultrafast electromechanical switches. *IEEE Transactions on Power Delivery*. 2015. Vol. 30. No 3. Pp. 1104-1109. DOI: <https://doi.org/10.1109/TPWRD.2014.2362996>.
7. Vilchis-Rodriguez D.S., Shuttleworth R., Smith A.C. et al. A comparison of damping techniques for the soft-stop of ultra-fast linear actuators for HVDC breaker applications. The 9th International Conference on Power Electronics, Machines and Drives (PEMD), Liverpool, UK, 2018. Pp. 1-6.
URL: https://www.research.manchester.ac.uk/portal/files/68110674/Soft_stop_techniques_full_paper_Final.pdf. (Accessed at 25.06.2000)
8. Soda R., Tanaka K., Takagi K., Ozaki K. Simulation-aided development of magnetic-aligned compaction process with pulsed magnetic field. *Powder Technology*. 2018. Vol. 329. No 15. Pp. 364-370. DOI: <https://doi.org/10.1016/j.powtec.2018.01.035>.
9. Horozha K.A., Podoltsev O.D., Troshchinsky B.A. Electromagnetic processes in a pulsed electrodynamic emitter for the excitation of elastic vibrations in concrete structures. *Tekhnichna Elektrodynamika*. 2019. No 3. Pp. 23-28. DOI: <https://doi.org/10.15407/techned2019.03.023>. (Ukr).
10. Bolyukh V.F., Oleksenko S.V., Shchukin I.S. Comparative analysis of linear pulse electromechanical converters electromagnetic and induction types. *Tekhnichna Elektrodynamika*. 2016. No 5. Pp. 46-48. DOI: <https://doi.org/10.15407/techned2016.05.046> (Rus).
11. Bolyukh V.F., Kashanskiy Yu.V., Shchukin I.S. Comparative analysis of power and speed indicators of linear pulse electromechanical converters of electrodynamic and induction types. *Tekhnichna Elektrodynamika*. 2019. No. 6. Pp. 35-42. DOI: <https://doi.org/10.15407/techned2019.06.035> (Rus).
12. Bolyukh V.F., Vinnichenko A.I. Concept of an induction-dynamic catapult for a ballistic laser gravimeter. *Measurement Techniques*. 2014. Vol. 56. Issue 10. Pp. 1098-1104. DOI: <https://doi.org/10.1007/s11018-014-0337-z>.
13. Ivashin V.V., Ivannikov N.A. Induction-dynamic drive. *Patent Russian Federation*. 2013. No 2485614 (Rus).
14. Fan G., Wang Y., Xu Q., et al. Design and analysis of a novel three-coil reconnection electromagnetic launcher. *IEEE transactions on plasma science*. 2019. Vol. 47. No. 1. Pp. 814-820. DOI: <https://doi.org/10.1109/TPS.2018.2874287>.
15. Bolyukh V.F., Katkov I.I. Influence of the form of pulse of excitation on the speed and power parameters of the linear pulse electromechanical converter of the induction type. *Proceedings ASME.*, Salt Lake City, Utah, USA, November 11-14, 2019, vol. 2B: Advanced Manufacturing. No: IMECE2019-10388, V02BT02A047, 8 p. DOI: <https://doi.org/10.1115/IMECE2019-10388>.
16. Zhou Y., Huang Y., Wen W. et al. Research on a novel drive unit of fast mechanical switch with modular double capacitors. *Journal of Engineering*. 2019. Vol. 2019. Issue 17. Pp. 4345-4348. DOI: <https://doi.org/10.1049/joe.2018.8148>.

ЗБУДЖЕННЯ ІМПУЛЬСНОГО ЕЛЕКТРОМЕХАНІЧНОГО ПЕРЕТВОРЮВАЧА ЕЛЕКТРОДИНАМІЧНОГО ТИПУ ВІД ДВОСЕКЦІЙНОГО ЄМНІСНОГО НАКОПИЧУВАЧА ЕНЕРГІЇ

В.Ф. Болюх

Національний технічний університет «Харківський політехнічний інститут»,

вул. Кирпичева, 2, Харків, 61002, Україна,

e-mail: vfbolyukh@gmail.com

Розроблено математичну модель імпульсного електромеханічного перетворювача (ІЕП) електродинамічного типу, в якій рішення рівнянь представлені у рекурентному вигляді, що під час чисельній реалізації дає змогу врахувати взаємозалежні електричні, магнітні, механічні та теплові процеси і їхні нелінійні параметри. За збереження загальної енергії імпульсного джерела встановлено вплив розподілу енергії між двома секціями ємнісного накопичувача енергії (ЄНЕ) і напруги, при якій підключається додаткова секція ЄНЕ. Під час роботи у прискорювальному режимі найбільша амплітуда електродинамічних зусиль (ЕДЗ) і максимальна швидкість мають місце у базовому варіанті ІЕП, що збуджується тільки від основної секції ЄНЕ, а найбільш ефективним є ІЕП з найменшою ємністю основної секції ЄНЕ, причому його максимальна величина в 2.61 вище, ніж у базового варіанту ІЕП. Під час роботи в ударно-силовому режимі у порівнянні з базовим варіантом ІЕП амплітуда ЕДЗ зменшується. Найбільш ефективним є ІЕП з найменшою ємністю основної секції ЄНЕ, причому його максимальна величина в 5.17 вище, ніж у базового варіанта ІЕП. У процесі експериментальних досліджень ІЕП в ударно-силовому режимі встановлено, що осцилограми напруги ЄНЕ і струму ІЕП відповідають розрахунковим характеристикам, а їхні основні показники з точністю до 5-7% узгоджуються між собою. Бібл. 16, рис. 6.

Ключові слова: імпульсний електромеханічний перетворювач електродинамічного типу, математична модель, дві секції ємнісного накопичувача енергії, критерій ефективності, експериментальні дослідження.

Надійшла 31.08.2020
Остаточний варіант 21.12.20